11-15-2002

Effect of Mosaicity in X-Ray Studies of Critical Behavior at the Nematic To Smectic-A Transition

Andrew Primak

Michael Fisch

Satyendra Kumar
Kent State University - Kent Campus, skumar@kent.edu

Effect of mosaicity in x-ray studies of critical behavior at the nematic to smectic-*A* transition

Andrew Primak,[1] Michael Fisch,[2] and Satyendra Kumar[1]
[1]*Department of Physics, Kent State University, Kent, Ohio 44242*
[2]*Liquid Crystal Institute, Kent State University, Kent, Ohio 44242*
(Received 21 May 2002; published 19 November 2002)

Previous studies of critical behavior at the nematic to smectic-*A* transition by high-resolution x-ray scattering were performed using low magnetic fields of 0.1–0.8 T. In those studies, the transverse resolution was limited by the sample mosaicity which complicated data analysis. In order to understand the effect of sample mosaicity on the measured values of critical exponents, the divergence of the smectic order correlation lengths $\xi_{\parallel,\perp}$ and susceptibility σ_o was studied in a magnetic field ranging from 0.25 to 5 T. The use of high (5 T) field reduced the sample mosaicity and improved the effective transverse resolution by almost two orders of magnitude. Three liquid crystals, two mixtures of 6th and 7th homologs of 4,4′-dialkylazoxybenzene (DnAOB) and 4-n-octylcyanobiphenyl (8CB) were studied. 15 wt% (D6.15AOB) and 40 wt% (D6.4AOB) mixtures of D7AOB in D6AOB have a wide nematic range, while 8CB has a narrow nematic range. Analysis of the data at different fields revealed a different and proper way to apply the mosaicity correction. The Gaussian mosaicity correction was found to be temperature independent but significantly ($\sim$3.5 times) smaller than the width of the sharpest $q_\perp$-scan, which has traditionally been used for mosaicity correction in all previous studies. The values of the critical exponents measured over almost four decades of reduced temperature were: $\nu_\parallel = 0.79 \pm 0.02$, $\nu_\perp = 0.69 \pm 0.02$, $\gamma = 1.46 \pm 0.04$ for D6.15AOB; $\nu_\parallel = 0.79 \pm 0.02$, $\nu_\perp = 0.67 \pm 0.02$, $\gamma = 1.44 \pm 0.04$ for D6.4AOB; and $\nu_\parallel = 0.70 \pm 0.02$, $\nu_\perp = 0.52 \pm 0.02$, $\gamma = 1.24 \pm 0.04$ for 8CB. The results for the two mixtures suggest that in wide temperature range nematics, far from the tricritical point, the exponents may be material independent. No significant effects of mosaicity on the values of the coefficient *c* of the fourth-order term in the structure factor were observed.

DOI: 10.1103/PhysRevE.66.051707 PACS number(s): 64.70.Md, 61.10.−i, 61.30.Eb

I. INTRODUCTION

Liquid crystals can be simply described as anisotropic fluids. A wide variety of phases and phase transitions are exhibited by liquid crystals. These transitions are physical realizations of a number of unique systems for which theoretical predictions have been made. One of the most interesting and most extensively studied phase transitions is the nematic to smectic-*A* (NA) transition. It is an example of a simple transition at which a system freezes (melts) in one dimension. However, after three decades of intense research on this topic, the NA transition still remains poorly understood. One of the serious problems is our inability to obtain reliable quantitative structural information in the close vicinity of the transition due to poor transverse resolution, which is determined by the sample mosaicity. In this paper, we report the results of a high-resolution x-ray diffraction study of the NA transition under a high (5T) magnetic field. The use of a high-field improved the effective transverse resolution by almost two orders of magnitude over previous studies and allowed us to obtain results, which were essentially *free of mosaicity effects*. The low-field data, analyzed without mosaicity correction, clearly demonstrated the artifact of mosaicity, which could be mistakenly attributed to crossover behavior. Using high-field mosaicity-free results as a reference revealed a different and proper way to correct the low-field data for the effects of mosaicity.

This paper has five sections. The following section gives a background of the NA transition and briefly reviews existing theoretical models and associated critical behavior. The structure factor for smectic fluctuations above the transition and a sample mosaicity are discussed in Sec. III. Sec. IV provides experimental details including the x-ray spectrometer, sample alignment, temperature control, and the methodology used. The results are presented and discussed in the last section and are followed by conclusions.

II. BACKGROUND

The nematic (*N*) phase has orientational but no translational order with long molecular axes aligned, on average, parallel to the unit vector $\hat{n}$ called the director. The conventional nematic order parameter is a symmetric traceless tensor [1],

$$Q_{ij} = S\left(n_i n_j - \frac{1}{3}\delta_{ij} \right),$$

where $S = \langle \frac{3}{2}\cos\theta - \frac{1}{2} \rangle$, θ is the angle between the long molecular axis and the director, $\langle \cdots \rangle$ means statistical averaging over all molecules and $n_\alpha (\alpha = x,y,z)$ are the director's components in the laboratory frame. The magnitude *S* provides a measure of the degree of orientational order.

At the NA transition, the continuous translational symmetry of the nematic phase is broken, which results in condensation of a one-dimensional density wave $\rho(z)$ along $\hat{z} \| \hat{n}$ and formation of the smectic-*A* (SmA) phase. Near the transition, the density wave is often approximated by a simple sine wave. The SmA order parameter is the coefficient Ψ of the spacially dependent term in the Fourier series expansion of $\rho(z)$ with period *d* equal to the smectic layer spacing [1];

$$\rho(z) \simeq \rho_o\{1+\mathrm{Re}[\Psi e^{iq_o z}]\},$$

where $q_o = 2\pi/d$ and ρ_o is the density in the nematic phase where Ψ is equal to zero.

Therefore, Ψ can be represented as a complex number

$$\Psi = |\Psi| e^{-iq_o u},$$

where $|\Psi|$ is the amplitude of the translational order, while the phase factor $(q_o u)$ defines the position of the smectic layers.

Using a phenomenological Landau approach, de Gennes [2] wrote the following expression for the SmA free energy

$$F_{NA} = \frac{1}{2}\int d^3r \left\{ a|\Psi|^2 + \frac{b}{2}|\Psi|^4 + c_\parallel |\nabla_\parallel \Psi|^2 + c_\perp |(\vec{\nabla}_\perp - iq_o \delta\hat{n})\Psi|^2 \right\} + F_N(K_i), \quad (1)$$

where a, b, and $c_{\parallel,\perp}$ are typical Landau expansion coefficients with the gradient term having different contributions from the directions parallel and perpendicular to smectic layers; $F_N(K_i)$ is the Frank elastic energy of director fluctuations [3]

$$F_N(K_i) = \frac{1}{2}\int d^3r \{K_1(\vec{\nabla}\cdot\hat{n})^2 + K_2(\hat{n}\cdot\vec{\nabla}\times\hat{n})^2 + K_3[\hat{n}\times(\vec{\nabla}\times\hat{n})]^2\}.$$

Here $K_i = K_i^o + \delta K_i$, where K_i^o's are the bare values of the splay, twist, and bend elastic constants.

There are several factors complicating the nature of the NA transition compared to the other transitions which are also described in terms of a two component complex order parameter. First of all, the coupling between the orientational and translational orders, so-called Ψ-S coupling, can change the sign of the fourth-order coefficient b in Eq. (1) and drive the NA transition first order [1]. The crossover from critical to tricritical and then to first-order behavior with decreasing nematic range was also predicted within the framework of microscopic mean-field theory by McMillan [4] and Kobayashi [5]. Another very important feature of the NA transition is the coupling between Ψ and nematic director fluctuations, or the $\delta\hat{n}$-Ψ coupling. Inclusion of this coupling described by $c_\perp|(\vec{\nabla}_\perp - iq_o\delta\hat{n})\Psi|^2$ in the SmA free energy allowed de Gennes to recognize the analogy between Eq. (1) and the Landau-Ginzburg free energy for superconductors [2]. Using this analogy Halperin, Lubensky, and Ma [6] predicted that the NA transition should always be at least weakly first order. The superconductor analogy, however, is not complete because of the broken gauge invariance [7] and the absence of true long-range order in the smectic phase due to the Landau-Peierls instability [8,9].

In spite of these complications, the NA transition was, at first, expected to be in the $3d$-xy universality class [2]. However, experimental observations [10] contradicted this prediction and indicated a profound effect of the two couplings on the nature of the transition. Two major features of this transition are nonuniversal critical behavior and weak anisotropy in the critical exponents $\nu_{\parallel,\perp}$ describing divergence of the correlation lengths $\xi_{\parallel,\perp} = \xi^o_{\parallel,\perp} t^{-\nu_{\parallel,\perp}}$ in the directions parallel and perpendicular to smectic layer normal. Here, $t = (T - T_{NA})/T_{NA}$ is the reduced temperature, T_{NA} is the transition temperature, and $\xi^o_{\parallel,\perp}$ are the bare correlation lengths. Several different theoretical approaches, mostly based on the Landau-de Gennes free energy, were developed in attempts to resolve these issues. Monte Carlo studies of the lattice model [11,12] suggest that the NA transition should be in the inverted $3d$-xy universality class with isotropic ($\nu_\parallel = \nu_\perp = \nu_{xy}$) critical exponents. On the other hand, the dislocation-mediated melting theory [13] predicts strongly anisotropic behavior ($\nu_\parallel = 2\nu_\perp$), in agreement with the existence of a $\nu_\parallel = 2\nu_\perp$ fixed point in the anisotropic scaling theory [14]. Gauge transformation theory [15] predicts different divergences of correlation lengths measured by x-ray diffraction and light scattering and predicts that the x-ray correlation lengths should display a crossover from isotropic ($\nu_\parallel = \nu_\perp = \nu_{xy}$) to strongly anisotropic ($\nu_\parallel = 2\nu_\perp$) divergence. Self-consistent one-loop calculations [16] predict a gradual crossover from isotropic to strongly anisotropic ($\nu_\parallel = 2\nu_\perp$) behavior, and a broad region of weak anisotropy ($1 \leqslant \nu_\parallel/\nu_\perp \leqslant 4/3$) consistent with experimental observations. Finally, Garland *et al.* [17] showed that possible corrections-to-scaling terms also could play an important role in describing critical behavior at the NA transition. Though some aspects of experimental results agree with predictions of one or another model, none of the existing theories can explain all features of the results [10] obtained by x-ray diffraction, light scattering, and heat capacity measurements.

III. SMECTIC STRUCTURE FACTOR, SAMPLE MOSAICITY, AND DATA ANALYSIS

Our theoretical understanding of the NA transition, as described in the preceding section, is very complicated, quite controversial, and far from complete. This emphasizes the importance and need for reliable, high-precision experimental measurements, which would help one select the most appropriate theoretical approach. Experimental data in the close vicinity of the transition is of special interest, since a crossover to strongly anisotropic behavior ($\nu_\parallel = 2\nu_\perp$) in this region is predicted by some models [15,16]. One of the sources of reliable results is high-resolution x-ray diffraction experiments, which directly probe the smectic density fluctuations in the nematic phase. However, to extract correct values of the smectic order correlation lengths and susceptibility, one has to know both, the structure factor and the experimental resolution. The latter is strongly affected by the sample mosaicity in the vicinity of the transition.

Using the harmonic approximation and neglecting the thermal fluctuations of the director, one obtains a simple Lorentzian form for the structure factor of smectic fluctuations in the nematic phase [1]. However, McMillan [18] observed a non-Lorentzian behavior of the x-ray scattering profile in the $q_\perp$ direction. He also reported anisotropy of the critical exponents for the correlation lengths. These interest-

ing features were later confirmed in all x-ray studies of the critical behavior at the NA transition.

In a later study with significantly improved instrumental resolution and temperature stability, Als-Nielsen *et al.* [19] found that the x-ray scattering data were adequately described by the following modified Lorentzian structure factor

$$S(\vec{q}) = \frac{\sigma_o}{1+\xi_\parallel^2(q_\parallel - q_o)^2 + \xi_\perp^2 q_\perp^2 + c\xi_\perp^4 q_\perp^4} \tag{2}$$

convoluted with the instrumental resolution function. Here σ_o is the susceptibility of the smectic order parameter, which diverges at the transition with the critical exponent γ, so $\sigma_o = \sigma_o^o t^{-\gamma}$ (σ_o^o is the bare value). Als-Nielsen *et al.* showed that the empirical fourth-order correction term with freely adjustable parameter c improved the goodness-of-fit parameter χ^2 for the transverse scan by 10–30 times and could be as large as 10% of the second term in $q_\perp$. They suggested that the large fourth-order corrections originated from splay-mode director fluctuations and represent a precursor to the anticipated $q_\perp^{-4+2\eta}$ line shape in the smectic phase [20]. The structure factor of Eq. (2) became well established and was used in the majority of subsequent x-ray studies of the NA transition [10].

In some studies [21,22], the x-ray data were also fit to an alternative form of the structure factor given by a Lorentzian raised to the power $1-\eta_\perp/2$ along the transverse direction

$$S(\vec{q}) = \frac{\sigma_o}{\xi_\parallel^2(q_\parallel - q_o)^2 + (1+\xi_\perp^2 q_\perp^2)^{1-\eta_\perp/2}}, \tag{3}$$

where $-2 < \eta_\perp < 0$ is an empirical exponent that is freely adjustable in the fits. Both Eqs. (2) and (3) have four adjustable parameters with weakly temperature dependent parameters c or $\eta_\perp$ reflecting a crossover in the transverse line shape, which changes from Lorentzian squared ($c \simeq 0.25, \eta_\perp \simeq -2$) at large t to Lorentzian-like ($c \lesssim 0.001, \eta \simeq 0$) at small t near T_{NA} [22]. The experimental data studied in Refs. [21,22] were fit equally well with both equations and the critical exponents were found to be essentially the same for both line shapes. Moreover, Nounesis *et al.* [22] showed that even using Eq. (2) with fixed value $c=0$ does not change the values of $\nu_{\parallel,\perp}$ and γ. Thus, they concluded that the precise line shape used in describing a non-Lorentzian correction to the x-ray scattering profile has no significant effect on the values of the critical exponents. A similar conclusion was made by Chan *et al.* [23], who used a slightly different form of Eq. (3) to analyze the x-ray data.

A somewhat different approach was used by Bouwman and de Jeu [24] to account for the non-Lorentzian profile of the transverse x-ray scans. Following the assumption introduced by Als-Nielsen *et al.* [19], they attributed the fourth-order correction in the transverse direction to splay-mode director fluctuations. It was argued that the temperature dependent line shape results from the competition between the terms $c_\perp|(\vec{\nabla}_\perp - iq_o\delta\hat{n})\Psi|^2$ and $K_1(\vec{\nabla}\cdot\delta\hat{n})^2$ in Eq. (1) for the smectic free energy. Close to T_{NA}, the $c_\perp|(\vec{\nabla}_\perp - iq_o\delta\hat{n})\Psi|^2$ term should become very small (since it disappears in the smectic phase) and the line shape should be dominated by the quartic term originating from $K_1(\vec{\nabla}\cdot\delta\hat{n})^2$. On the other hand, further away from T_{NA}, the above assumption is not valid and the contribution of the $\xi_\perp^2 q_\perp^2$ term originating from $c_\perp|(\vec{\nabla}_\perp - iq_o\delta\hat{n})\Psi|^2$ becomes more important. Thus, it can be concluded [24] that, for a given $q_\perp$, the contribution of the quartic term becomes dominant close to T_{NA}. This is quite opposite to the earlier discussed statement from [21,22] that the transverse line shape changes from a Lorentzian near T_{NA} to a Lorentzian squared at large t. This statement was based on the small value of the parameter c in the vicinity of T_{NA}. For that reason, a modified form of the structure factor, different from Eq. (2) in the quartic term, was used [24]

$$S(\vec{q}) = \frac{\sigma_o}{1+\xi_\parallel^2(q_\parallel - q_o)^2 + \xi_\perp^2 q_\perp^2 + \xi_s^4 q_\perp^4}. \tag{4}$$

Here, the magnitude of the quartic term is given explicitly by an independent correlation length ξ_s (s for splay), which is assumed to diverge with its own critical exponent ν_s. It is important to note that this approach is equivalent to using the $c\xi_\perp^4 q_\perp^4$ term with c as a free parameter, since Eqs. (2) and (4) are algebraically identical with $\xi_s = c^{1/4}\xi_\perp$. Indeed, Nounesis *et al.* [22] showed that the temperature dependence of $c^{1/4}\xi_\perp$ can be fit nicely by a single power law. Since both approaches are equivalent, the contradiction mentioned above in the interpretation of the temperature behavior of the transverse line shape is artificial. However, it was claimed [24] that fixing c at its average value or at zero gives rise to noticeably larger values of the critical exponents. Their values obtained with $c=0$ increased from 0.82 to 0.93 for $\nu_\parallel$, from 0.58 to 0.74 for $\nu_\perp$, and from 1.38 to 1.64 for γ compared to the values obtained when c was left free. This disagrees with the results [22,23] mentioned earlier, where no significant change of the values of the critical exponents was observed.

To conclude, the empirical structure factor given by Eq. (2) has the simplest form and it quite adequately describes the experimental x-ray profiles. Currently, there is no theory which predicts this precise form of the transverse line shape. For that reason, the introduction of an independent correlation length ξ_s does not seem to be justified and would only further complicate the matter.

Knowing the correct form of the structure factor is necessary but not sufficient to obtain reliable values of the correlation lengths and susceptibility. The experimental resolution has to be taken into account in the data analysis to extract $\xi_{\parallel,\perp}$ and σ_o. In the close vicinity of the transition, the resolution function becomes especially important. For example, Als-Nielsen *et al.* [19] first claimed that the critical exponents $\nu_\parallel$ and $\nu_\perp$ were identical and exhibited a crossover from $3d$-xy to mean-field values on approaching T_{NA}. However, these conclusions did not remain valid, when the correct form (Lorentzian) of the longitudinal resolution function was used to reanalyze the data.

The effective resolution function in an x-ray scattering experiment near the NA transition depends on two factors. The first comes from the instrumental resolution of the x-ray

spectrometer and the second from the imperfect alignment of the sample. The layers in different (fluctuating) correlated volumes (domains) of the incipient smectic phase in the nematic phase are not perfectly parallel to each other but have a finite distribution, which is referred to as mosaic distribution or the mosaicity.

In x-ray experiments, longitudinal ($q_\parallel$) and transverse ($q_\perp$) scans are performed above the NA transition. During a $q_\parallel$-scan, both the sample and the detector are rotated simultaneously, so the detector measures scattering from the set of smectic domains which satisfy the Bragg condition. Since the width of the $q_\parallel$-scan is proportional to $\xi_\parallel^{-1}$ [see Eq. (2)], it decreases as T approaches T_{NA} until it reaches the value of the longitudinal instrumental resolution, $\Delta q_\parallel$. On the other hand, the sample is rotated during a $q_\perp$-scan to affect lateral changes in $\vec{q}$. Far from T_{NA}, where the mosaicity effect is small, the width of the $q_\perp$-scans is roughly proportional to $\xi_\perp^{-1}$ [see Eq. (2)]. However, close to T_{NA} the mosaicity becomes significant and the width of $q_\perp$-scans saturates at the mosaicity limit, say, Δq_M, rather than at the instrumental transverse resolution $\Delta q_\perp$. Since typical high-resolution x-ray spectrometers have $\Delta q_\perp \lesssim 10^{-5}$ Å^{-1}, the effective transverse resolution in the scattering plane is always determined by the sample mosaicity. Thus, the mosaicity sets the lower boundary on the reduced temperature below which reliable values of $\xi_{\parallel,\perp}$ and σ_o can no longer be obtained.

All previous x-ray studies [10] of critical behavior near the NA transition have been performed in a magnetic field range $B \sim 0.1$–0.8 T with the reported values of the mosaicity full width at half maximum (FWHM) (Δq_M) varying from 1.7° (6×10^{-3} Å^{-1}) [25] to 0.1° (4×10^{-4} Å^{-1}) [26]. These values are substantially larger than the instrumental transverse resolution $\Delta q_\perp \sim 10^{-5}$ Å^{-1}. In the first study [25], low magnetic fields $B \simeq 0.08$ T and $B \simeq 0.18$ T were used to align the samples. The mosaic width was estimated from the limiting transverse line width as $t \to 0$ and was assumed to be temperature independent for $t > 0$. Davidov *et al.* [25] mentioned that the last assumption was likely a poor approximation far from T_{NA}. The mosaicity profile was modeled by a Gaussian of the corresponding width and included in the data analysis to deconvolve the structure factor. The correction was found to be negligible over the complete temperature range ($5\times10^{-5} < t < 1\times10^{-3}$) for the 0.18 T experiment. However, it was substantial for $t < 2\times10^{-4}$ for the 0.08 T measurements.

Mosaicity was also taken into account by Chan *et al.* [23] who used a 0.45 T aligning field. They argued that the narrowest observed mosaicity ($0.4° \simeq 9\times10^{-4}$ Å^{-1} FWHM) remains unchanged in the nematic phase. This argument was based on the assumption that the precise sample alignment at or above the transition temperature, though unknown, should depend only on the uniformity of the magnetic field. The Gaussian mosaicity correction used in Ref. [23] affected the points where $\xi_\perp^{-1}$ was less than or comparable to the mosaicity width. However, the corrected results did not improve the power-law fits and, in fact, made them slightly worse. In addition, when the transition temperature was allowed to vary, the critical exponents became identical to the values obtained without mosaicity corrections. From these findings Chan *et al.* concluded that corrections for mosaicity were smaller than the precision of their experiments.

The *insignificance* of mosaicity corrections was also reported in several other papers. Kortan *et al.* [26] observed a mosaicity range from 0.1° to 0.4° in a 0.4 T field. They conclude that the correction for mosaicity did not alter the results when the mosaicity was less than $0.001q_o$ ($q_o = 0.0206$ Å^{-1}) and only affected the points closest to T_{NA}. Ocko *et al.* [21] performed experiments with various aligning field strengths (0.6–0.8 T) for some of the samples. They concluded that the critical behavior in the nematic phase did not depend on the field strength, although the mosaicity in the smectic phase did. Therefore, they assumed that the effects of mosaicity in the nematic phase can be neglected. Chen *et al.* [27] reported the mosaicity widths 2.24° (9.2×10^{-3} Å^{-1}), 0.72° (3.0×10^{-3} Å^{-1}) and 0.26° (1.1×10^{-3} Å^{-1}) for their three samples studied in a 0.25 T field. They applied a Gaussian mosaicity correction for the 0.72° mosaicity sample. The exponents obtained after mosaicity correction were essentially identical to those for the sharpest mosaicity (0.26°) but without using mosaicity correction.

Unlike the results discussed above, Bouwman and de Jeu [24] indicated that correction for the mosaicity has a strong influence on the extracted parameters. They studied the NA transition for two different materials in a 0.4 T field and obtained the mosaicity values of 0.4° (1.5×10^{-3} Å^{-1}) for one and 0.56° (2.0×10^{-3} Å^{-1}) (for a different sample). Since the experimental mosaicity profiles were well described by a Lorentzian, Bouwman, and de Jeu used a Lorentzian rather than Gaussian mosaicity correction. The corrected values of the critical exponents for the material with the wider mosaicity of 0.56° increased from 0.82 to 0.91 for $\nu_\parallel$ from 0.58 to 0.72 for $\nu_\perp$ and from 1.38 to 1.62 for γ. The corrections for the material with narrower mosaicity (0.4°) affected only the values of $\nu_\perp$ and γ. Concerned with the large effects of mosaicity corrections, Bouwman and de Jeu questioned the validity of the assumption that the sharpest mosaicity observed remains unchanged in the nematic phase. They argued that the mosaicities in the two phases have different origins. The mosaicity in the smectic phase is caused by effects of the boundaries penetrating into the bulk of the sample. On the other hand, the penetration length for defects in the nematic phase is of the order of microns and the mosaicity in the nematic phase should only depend on the nonuniformity of the magnetic field. Thus, the director distribution in the nematic phase should be close to zero, while the limiting linewidth of a $q_\perp$-scan should depend on temperature gradients in the sample. Using these arguments Bouwman and de Jeu concluded that the measured mosaicity is an overestimation.

So far, we have only discussed the consequences of the mosaicity correction on the values of the critical exponents. A different effect of the mosaicity on the line shape of transverse x-ray scans was pointed out by Dasgupta [12]. During time evolution of his Monte Carlo simulation of the NA transition, parts of the system sometimes fluctuate into the vicinity of one of the ground states corresponding to small global

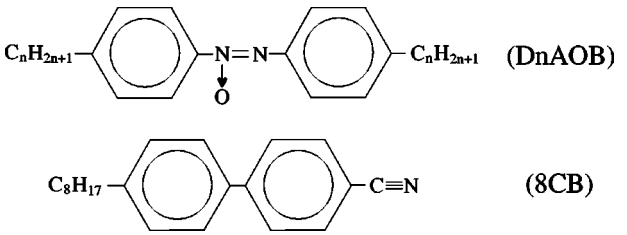

FIG. 1. Chemical formulas of 4,4′-dialkylazoxybenzene (DnAOB) homologous series and 4-*n*-octylcyanobiphenyl (8CB).

rotations of the system. These fluctuations cause the simulated correlation function $g(q_\perp)$ to fall off faster than a Lorentzian for relatively large values of $q_\perp$ while $g(q_\parallel)$ remains unaffected. Dasgupta showed that the imposition of constraints, which suppress these fluctuations, brings $g(q_\perp)$ closer to the Lorentzian form and also causes an increase in $\xi_\perp$. He suggested that similar effects in real systems may be produced by the sample mosaicity. He argued that the effect of averaging over a sample with finite mosaic distribution would essentially be the same as that of time averaging during evolution where parts of the system undergo small uniform rotations. He also claimed that convoluting a Lorentzian with a Gaussian mosaicity function produces the lineshape in experiments. Based on this analysis, it was suggested that a careful experimental study of the effects of mosaicity should provide important insight into the puzzling critical behavior at the NA transition.

IV. EXPERIMENTAL DETAILS

In our study, we used two mixtures of the sixth and seventh members of the 4,4′-dialkylazoxybenzene (DnAOB) homologous series, as well as 4-*n*-octylcyanobiphenyl (8CB). Their chemical formulas are shown in Fig. 1. The three members of the DnAOB series (n=6,7,8), which are also referred to as D6AOB, D7AOB, and D8AOB exhibit a simple isotropic-*N*-SmA phase sequence. The sixth homolog has the widest nematic range with $T_{NA}/T_{NI}=0.88$. Light scattering studies [28] of the twist elastic constant provide evidence that the NA transition in D6AOB is continuous to within at least 0.1 mK. The optical birefringence [29,30], diamagnetic susceptibility [31], and x-ray measurements [27] on D6AOB and D6AOB+D7AOB mixtures were also consistent with second-order behavior. However, the SmA phase in pure D6AOB is monotropic and addition of $\gtrsim 10\%$wt D7AOB is necessary to ensure the SmA phase stability required for x-ray measurements. We prepared 15 wt% (D6.15AOB) and 40 wt% (D6.4AOB) mixtures of D7AOB in D6AOB with $T_{NA}/T_{NI}=0.89$ and 0.91, respectively. Here, D6.xAOB represents a mixture of D6AOB and D7AOB, with *x* being the weight fraction of D7AOB. The results of a previous study [31] indicated that the NA transition becomes first order for approximately 46% concentration of D8AOB in D7AOB. Thus, both of our mixtures had the NA transitions well removed from the tricritical point and were good candidates for critical behavior studies. The NA transition in 8CB ($T_{NA}/T_{NI}=0.98$) is believed to be very close to the tricritical point [21,32] and perhaps weakly first order [33–36]. It was studied to compare the results of high-field measurements with previous results obtained by x-ray [21,25] and light scattering [37]. The values of T_{NA} for all three samples were in the convenient ~ 20–$30\,^\circ C$ range.

The x-ray scattering experiments were done using a 12 kW Rigaku RU-200 rotating anode generator, a two-circle Huber goniometer with a pair of Si (111) single crystals as monochromator and analyzer, and a 5 T superconducting magnet. A schematic diagram is presented in Fig. 2. $K\alpha$ lines emitted by the target (Cu or Mo) Bragg diffracted from the monochromator. Several *xy* slits were used to collimate the beam and define its crosscection. The slit S_3 before the magnet was also used to block the Cu $K\alpha_2$ line. This resulted in essential loss of intensity ($\sim 75\%$ due to partial overlapping of the two lines) but simplified the data analysis. Unfortunately, we could not block the Mo $K\alpha_2$ line as it was spatially too close to $K\alpha_1$ line and the loss of intensity was unacceptable. The monochromatic and well collimated x-ray beam impinged on the sample placed inside the oven inserted in the superconducting magnet. The magnet had a special split-coil design, which features horizontal field and two orthogonal horizontal bores. The x-ray beam passed through one of the bores, while the field was parallel to the axis of the second bore. The magnet was mounted on the θ circle of the two-circle Huber goniometer. The angles θ and 2θ were changed with a precision of $0.000\,25°$. X-ray photons scattered from the sample were Bragg reflected from the analyzer and counted with a Na(Tl)I scintillation detector. To avoid effects of any power fluctuations in the x-ray source, the intensity of the scattered beam was measured against the incident monochromatic beam flux.

The longitudinal resolution of the spectrometer was $\Delta q_\parallel \simeq 2\times 10^{-4}$ Å^{-1} FWHM. For the Cu target, the longitudinal resolution function has a single peak corresponding to the Cu $K\alpha_1$ line, which is well described by a sum of three Lorentzians [21] convoluted with the energy broadening Lorentz-

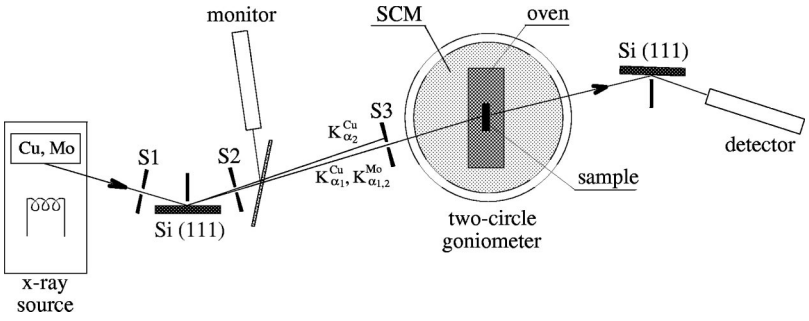

FIG. 2. The x-ray scattering setup.

ian. However, for the Mo target, both lines of the Mo $K\alpha_{1,2}$ doublet can be resolved because of dispersion at nonzero angles, and the longitudinal resolution was modeled by a sum of six Lorentzians. The transverse in-plane resolution is smaller by a factor of sin θ ($\sim$40 times for $\theta \sim 1.5°$) than the longitudinal resolution and can be approximated by a delta function. However, in practice, the resolution in the transverse direction is limited by the sample mosaicity rather than the instrumental resolution. The effective transverse resolution and, thus, the sample mosaicity, was measured and then used in the data analysis. The out-of-plane instrumental resolution can be modeled by the convolution of two square waves, which produces a trapezoidal function, usually approximated by a Gaussian [9,24]. Our calculations gave the Gaussian width $\sigma_z \simeq 4\times10^{-2}$ Å^{-1} for the Cu $K\alpha_1$ line and $\sigma_z \simeq 8\times10^{-2}$ Å^{-1} for the Mo $K\alpha$ doublet. In principle, the vertical resolution may also be affected by the sample mosaicity, which should have similar shape in all directions perpendicular to the aligning field. However, the mosaicity width is almost always negligible compared to the instrumental values of σ_z.

The sample, typically 1 mm thick and 6 mm in diameter, was sealed between two thin ($\sim 8\mu$m) Mylar sheets spaced with a Teflon O-ring. The Mylar windows and the *O*-ring were held between two aluminum plates, thus sealing the sample. The sample cell was placed inside a two-stage oven and the oven was inserted horizontally in the superconducting magnet. The sample was positioned exactly in the center of the magnet.

The sample was first heated to the isotropic phase and then cooled down slowly in the presence of a predetermined magnetic field to a temperature about 3 K above T_{NA}. In order to make measurements in different fields, the magnetic field was first lowered to 0 T, the sample temperature was then raised to the isotropic phase, and then the magnet charged to a new field. This precaution was necessary to avoid any possible memory (remnant alignment) effects in the sample.

The two-stage cylindrical oven, 5.5″ long and 1.9″ in diameter was specially designed to fit inside the 2″ magnet bore. The inner stage had beryllium windows and the outer stage openings were covered with thin Mylar films. Both stages were controlled independently by home-made temperature controllers. The temperature of the outer stage was set about 1° below T_{NA}, while the inner stage temperature was monitored and controlled by the computer during the experiment. The temperature stability was found to be $\lesssim \pm 1mK$ over a long term (24 h) and $\lesssim \pm 0.5$ mK over a short term (1 h).

The D6.15AOB sample had a phase transition temperature $\sim 20\,°$C, a few degrees below the room temperature. In order to control the temperature of this sample, two cooling coils made of thin copper tubing were inserted inside the magnet bore, one on each side of the oven. A refrigerated circulating bath was used to flow cold liquid at a constant temperature through the coils in order to lower the ambient temperature outside the oven to $\sim 15\,°$C.

Very near T_{NA} a sample temperature gradient should result in ''appearant'' coexistence of the *N* and SmA phases.

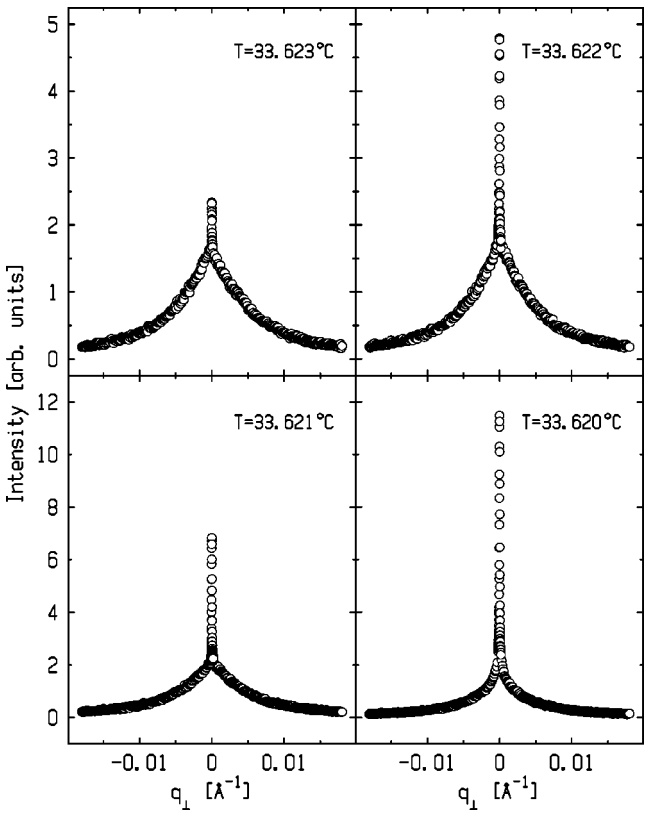

FIG. 3. Transverse in-plane scans for 8CB very near T_{NA} obtained using a one-stage oven without Be windows. The ''spikey'' appearance indicates the coexistence of the *N* and SmA phases, i.e., the presence of temperature gradients.

The scattering from the *N* phase and the quasi-Bragg scattering from the SmA phase give different contributions to $q_\perp$-scans. As a result, in the presence of large enough temperature gradient the $q_\perp$-scans should display a sharp smectic spike on top of a relatively broad nematic peak. If the gradients are larger than the temperature stability very near T_{NA}, $q_\perp$-scans for at least one temperature point should exhibit this ''spikey'' shape. The signature of such coexistence behavior was, indeed, observed in the preliminary studies done with a one-stage oven without Be windows (see Fig. 3). However, it has not been seen with the two-stage oven described above. Thus, we concluded that temperature gradients in our experiments were less than 0.1 mK/mm.

Small drift in the phase transition temperature was observed in all three samples and taken into account in the data analysis. The initial drift in the D6.15AOB sample was about 5 mK/day but stabilized at 0.5 mK/day for subsequent scans of this sample. The D6.4AOB sample had a T_{NA} drift of 3 mK/day for a large part of the measurements. Later it reduced to the same small rate $\sim$0.5 mK/day. Finally, the 8CB sample had the drift rate of 2 mK/day. This slight drift in transition temperatures could be related to sample decomposition.

V. RESULTS AND DISCUSSION

By charging the superconducting magnet at different currents we could vary the applied magnetic field over a large

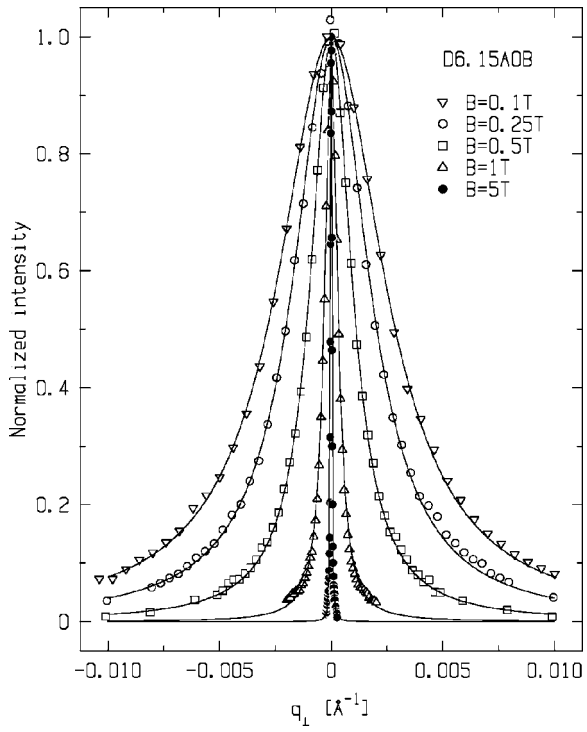

FIG. 4. The sharpest $q_\perp$-scans for D6.15AOB obtained at the temperature point closest to T_{NA} and normalized for comparison. These scans represent the effective transverse resolution at different fields. The solid lines are the fits to a triple Lorentzian (5 T) and a single Lorentzian (other fields).

0.25–5 T range and study the field dependence of the sample mosaicity. Figure 4 shows the sharpest $q_\perp$-scans at different fields for the D6.15AOB sample. These were recorded at the experimental temperature closest to T_{NA} and normalized for easy comparison. Since $\xi_\perp \to \infty$ at T_{NA} and the correlation function $S(q_\perp)$ [see Eq. (2)] becomes infinitely sharp, these scans represent the effective transverse resolution at different field strengths and their width $\Delta q_M(B)$ is closely related to the mosaicity width at the transition. It is important to note that the 5 T scan is several times sharper than the longitudinal resolution $\Delta q_\parallel$ and is essentially limited by the instrumental transverse resolution $[\Delta q_M(5T) \sim \Delta q_\perp]$. The 5 T scan was better fit by a triple Lorentzians just as the resolution limited $q_\parallel$-scan, while all other scans were reasonably well fit by a single Lorentzian. The use of a 5 T field improved the effective (mosaicity limited) transverse resolution by 80 times compared to a 0.1 T field used in Ref. [25] and by 60 times compared to a 0.25 T field used in Ref. [27]. Thus, the effects of sample mosaicity on the 5 T data were found to be negligible. However, the sample mosaicity became more important in low-field experiments.

To make this argument quantitatively, we found it reasonable to define the reduced temperature t_M, at which the effects of mosaicity become significant. As we have discussed, the scattering from smectic fluctuations in the nematic phase is well described by the structure factor $S(\vec{q})$ given by Eq. (2). The mosaicity effects have to be considered when the width of $S(q_\perp)$ (roughly proportional to $\xi_\perp^{-1}$) is comparable to Δq_M. Since $\xi_\perp$ is known to diverge as $\xi_\perp^o t^{-\nu_\perp}$, we can estimate t_M from the condition $\xi_\perp(t_M) \sim (\Delta q_M)^{-1}$, which gives $t_M \sim (\xi_\perp^o \Delta q_M)^{1/\nu_\perp}$. Thus, the mosaicity corrections become important and should be taken into account if $t \lesssim t_M$ is accessed during an x-ray experiment. On the other hand, they are expected to be insignificant for data points in the region $t > t_M$. We have to point out that for the typical value $\nu_\perp \sim 0.6$ the estimate gives $t_M(5\text{ T})/t_M(0.25\text{ T}) \sim [(\Delta q_M(5\text{ T})/\Delta q_M(0.25\text{ T})]^{1/\nu_\perp} \simeq (1/60)^{1/0.6} \simeq 10^{-3}$. Therefore, a 5 T field allows one to access three more decades of reduced temperature than a 0.25 T field. However, there are two more characteristic reduced temperatures in experiments. The first is the temperature stability ΔT of the oven ($t_s \sim \Delta T/T_{NA}$), while the second is related to the longitudinal instrumental resolution $\Delta q_\parallel$ and can be estimated as $t_\parallel \sim (\xi_\parallel^o \Delta q_\parallel)^{1/\nu_\parallel}$. The largest value out of t_s, t_M and $t_\parallel$ sets the lower boundary on the range of reduced temperature, where reliable data can be obtained.

The critical divergence of the correlation lengths and susceptibility in the D6.15AOB sample was studied under three different strengths of magnetic field (5 T, 0.5 T, and 0.25 T). The longitudinal $q_\parallel$-scans and in-plane transverse $q_\perp$-scans were performed over $\sim$3.5 decades of reduced temperature. To obtain reasonably good statistics the counting time varied from $\sim$6 h per scan far from T_{NA} ($t \sim 10^{-2}$) to $\sim$30 min per scan in the close vicinity of T_{NA} ($t \sim 10^{-5}$). The representative scans in the different regions of t for the 5 T experiment are shown in Fig. 5. The data were first analyzed without mosaicity correction by fitting both $q_\parallel$- and $q_\perp$-scans *simultaneously* to the convolution of the structure factor given by Eq. (2) with the instrumental resolution function. Data analysis was carried out with the commercial software packages C-PLOT [38] and Mathematica [39], which both produced almost identical results. The fitting parameters were the correlation lengths $\xi_{\parallel,\perp}$, the susceptibility σ_o, the fourth-order coefficient c, the smectic wave vector q_o (nearly temperature independent in our studies), and a constant background term. Fixing the values of q_o at the experimental value did not influence the fitting results. Using this procedure for every temperature, we obtained the temperature dependences of $\xi_{\parallel,\perp}$ and σ_o for different magnetic fields. The phase transition temperature was located with 1 mK precision by monitoring the width and the shape of the $q_\perp$-scans. Upon entering the SmA phase the alignment imposed by the magnetic field is distorted by thermal expansion and boundary effects penetrating into the bulk. As a result, the $q_\perp$-scans become slightly wider and often asymmetric immediately below T_{NA}. Thus, the transition was identified by the sharpest $q_\perp$ scan, while the appearance of the asymmetric shape (see Fig. 6) provided extra evidence for the system entering the SmA phase.

Figure 7 shows the log-log plots of the dimensionless quantities $q_o \xi_{\parallel,\perp}(t)$ and $\sigma_o(t)$. Here, the reduced temperature t was calculated using the experimental value of T_{NA}. The 5 T data fall on straight lines indicating simple power-law divergences, i.e., $\sigma_o = \sigma_o^o t^{-\gamma}$, $\xi_\parallel = \xi_\parallel^o t^{-\nu_\parallel}$, and $\xi_\perp = \xi_\perp^o t^{-\nu_\perp}$. As expected, no mosaicity effects were seen in the 5 T data, which are in $t \gg t_M \sim 10^{-8}$ regime. These data are free from the effects of sample mosaicity and represent the

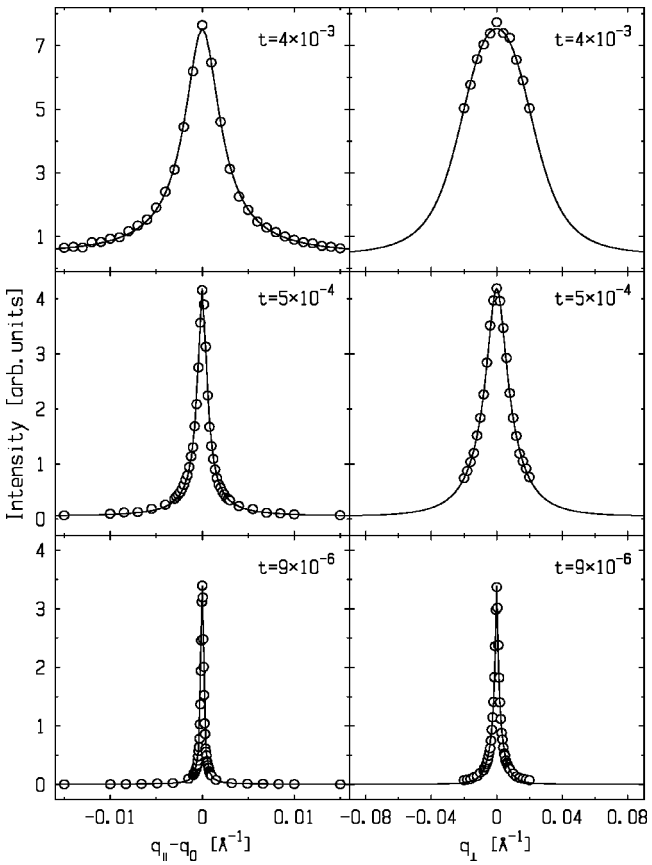

FIG. 5. Representative longitudinal $q_{\|}$- and transverse in-plane $q_{\perp}$-scans for D6.15AOB in a 5 T field at different values of the reduced temperature t. The solid lines are the fits to the structure factor Eq. (2) convoluted with the appropriate resolution function.

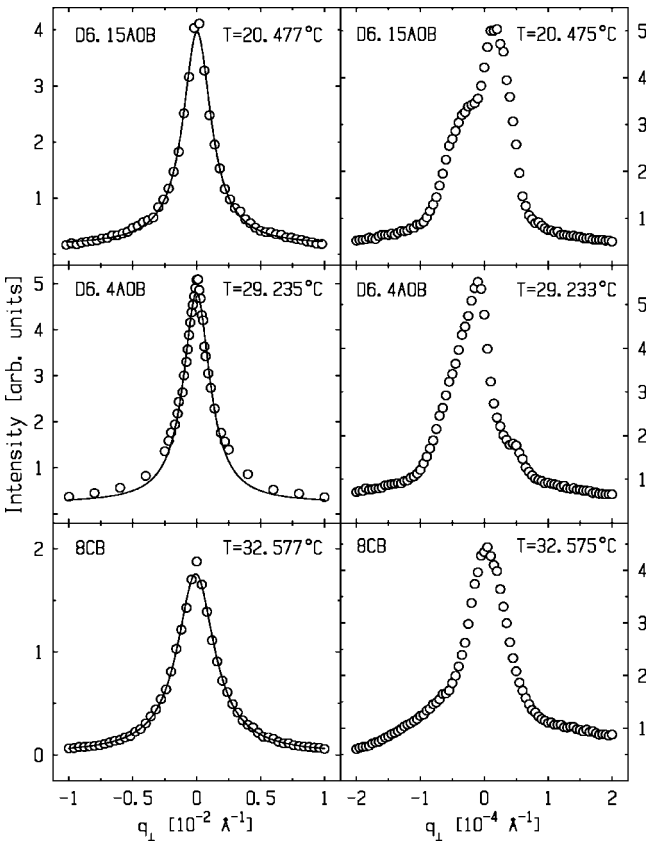

FIG. 6. The transverse in-plane $q_{\perp}$-scans for samples in a 5 T field very near the transition. The assymetry in shape is a clear indication of entering the smectic-*A* phase, where the sample develops domain structure. The solid Lorentzian lines are symmetry guides for the eye.

true divergence of the correlation lengths and the susceptibility. On the contrary, the low-field data at 0.5 T and 0.25 T clearly indicate the signature of mosaicity. Far from the transition, in $t>t_M$ region, the mosaicity effects are insignificant and the values of $\xi_{\|,\perp}$ and σ_o for high and low fields are the same. However, as one approaches the transition and enters the $t \lesssim t_M$ regime around $t \sim 10^{-5}$, the effects of mosaicity become important and cause the bending of the curves $\xi_{\|,\perp}(t)$ and $\sigma_o(t)$ away from the 5 T data. Similar behavior was also observed [21] in weekly first-order systems. However, our previous arguments and the 5 T results completely rule out this possibility for D6.15AOB. It is important to note that this bending is a pure artifact of sample mosaicity and has nothing to do with any type of crossover behavior.

The low-field data must be properly corrected for the mosaicity in order to ''unbend'' the curves and restore the true values of $\xi_{\|,\perp}(t)$ and $\sigma_o(t)$. One must be cautious against fitting the low-field data to straight lines and treating T_{NA} as a fitting parameter. This can artificially yield single power-law fits by forcing the best fit value of T_{NA}^{fit} to be significantly lower than the experimental value T_{NA}^{expt}. The larger the effect of mosaicity, the larger is the difference $\Delta T_{NA}=T_{NA}^{\text{expt}}-T_{NA}^{fit}$. For 5 T field, we found $\Delta T_{NA} \leqslant 0.5$ mK, which is well within experimental uncertainty. However, for the 0.25 T data the average value of ΔT_{NA} is about 3 mK and is much larger than the uncertainty in T_{NA}^{expt}. Clearly, fitting the mosaicity-affected results to straight lines with floating T_{NA} produces wrong transition temperatures. This causes the data points to shift to larger values of reduced temperature making it impossible to approach as close to the transition as allowed by the temperature stability (see Fig. 8). This seems to be the case in the majority of previous x-ray studies, where the data points were shown only for the range $t \gtrsim 10^{-5}$ with the reported temperature stability of 1 mK (or smallest $t \sim 3\times 10^{-6}$).

To correct the D6.15AOB data for the effects of the sample mosaicity, the smectic structure factor $S(\vec{q})$ was convoluted with the instrumental resolution function and the sample mosaicity modeled by a Gaussian. The Gaussian mosaicity width σ_M was first set to the width of the sharpest $q_{\perp}$-scans (i.e., $\sigma_M=\Delta q_M$) as it has been previously done [25,23,27]. The corrections for the 5 T data were found to be negligible, in full agreement with our expectations. On the other hand, the mosaicity correction with $\sigma_M=\Delta q_M$ applied to the low field data resulted in unexpectedly large changes in the values of the correlation lengths and the susceptibility. Not only the fits to the data very near T_{NA} produced extremely large values of $\xi_{\|,\perp}$ and σ_o with $\gtrsim 100\%$ uncertainties, but also the rest of the data were found to have unrealistically larger values of $\xi_{\|,\perp}$ and σ_o than the corresponding

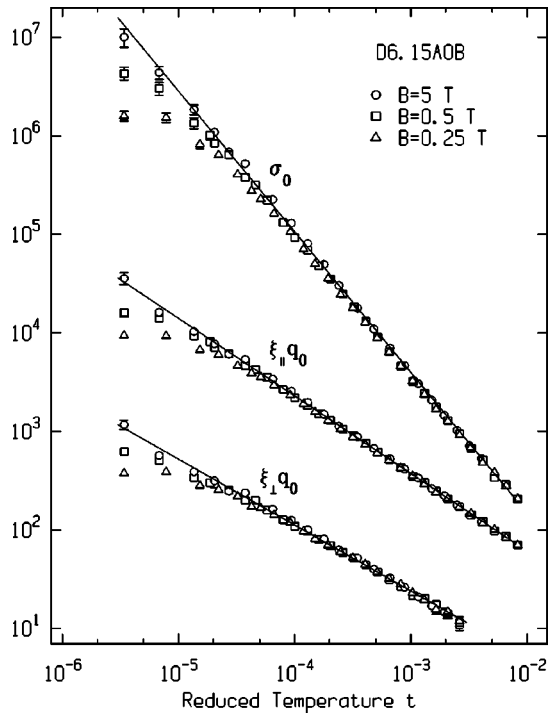

FIG. 7. Log-log plots of $q_o\xi_{\parallel,\perp}$ and σ_o vs reduced temperature t for D6.15AOB without a mosaicity correction at different fields ($q_o = 0.237$ Å^{-1}). The solid lines are the single power-law fits for the 5 T data only. The bending of the low-field data at $t \lesssim 10^{-5}$ is due to the mosaicity effect.

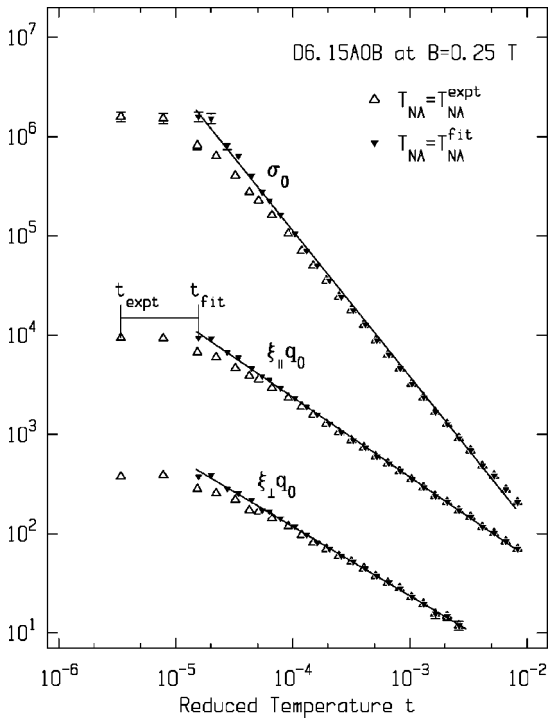

FIG. 8. Log-log plots of $q_o\xi_{\parallel,\perp}$ and σ_o vs $t=(T-T_{NA})/T_{NA}$ for D6.15AOB in a 0.25 T field without a mosaicity correction. Two sets of plots correspond to the values of T_{NA} determined from experiment T_{NA}^{expt} and from fits with floating T_{NA} (T_{NA}^{fit}). The solid lines are the single power-law fits with T_{NA}^{fit}. As the experimental curves are forced to ''unbend,'' the data points shift away from their true values on the t axis.

5 T values (see Fig. 9). These calculations indicate that fixing the mosaicity width σ_M from the sharpest $q_\perp$-scan is not a proper correction for the mosaicity. It is interesting to note very large effects of the mosaicity correction previously reported by Davidov *et al.* [25]. Bouwman and de Jeu [24] also obtained very large corrections for $\xi_\perp$ and σ_o which resulted in $\sim$10% increase in the values of $\nu_\perp$ and γ. In addition, Chan *et al.* [23] mentioned that the mosaicity correction did not improve the power-law fits, but made them worse. Clearly, previous researchers had encountered similar anomalies in data analysis.

Since the traditional $\sigma_M = \Delta q_M$ correction failed, we tried a different approach. We chose one data point in the vicinity of the transition and varied σ_M until the corrected values of $\xi_{\parallel,\perp}$ and σ_o became close to the corresponding values obtained with 5 T field. Once such a value of σ_M had been found, it was used to correct the rest of the data. Using this procedure, we obtained an excellent agreement (see Fig. 10) between the corrected low-field data and the mosaicity free 5 T data. In addition, the average values of T_{NA}^{fit} obtained with this method were less than 0.5 mK away from T_{NA}^{expt} giving us another half decade of useful data. However, the value of σ_M necessary to obtain such a good agreement was roughly 3.5 times smaller than measured Δq_M for both sets of the low-field (0.5 T and 0.25 T) data. Thus, our results support one of the previously used assumptions that the mosaicity width does not vary with temperature in the N phase, but reveal that the actual mosaicity width is significantly smaller than the width of the sharpest $q_\perp$-scan Δq_M. This is consistent with the Bouwman and de Jeu [24] assumption that the sharpest $q_\perp$-scan overestimates the mosaicity.

The values of the critical exponents obtained for the D6.15AOB sample were $\gamma = 1.46 \pm 0.04$, $\nu_\parallel = 0.79 \pm 0.02$, $\nu_\perp = 0.69 \pm 0.02$. The temperature dependences of $\xi_{\parallel,\perp}$ and σ_o are described well by single power-laws over $\sim$3.5 decades of reduced temperature. Reliable values of $\xi_\perp$ far away from the transition could not be obtained, because in this region the $q_\perp$-scans required a wide range of scattering angles which were not accessible because of the magnet bore dimensions. Though the truncated $q_\perp$ scans, fitted simultaneously with $q_\parallel$-scans, produced larger uncertainties in the values of $\xi_\perp$, they were very useful and helped to obtain correct values of $\xi_\parallel$ and σ_o. The reported errors in the exponents were estimated from temperature range shrinking. The values of $\nu_\parallel$ and $\nu_\perp$ appear to be slightly larger than but within the range of error bars of the values $\nu_\parallel = 0.75 \pm 0.05$ and $\nu_\perp = 0.65 \pm 0.05$ previously reported for a slightly different concentration D6.1AOB [27]. This small increase can be attributed to the different mosaicity correction. It is not reasonable to expect a large manifestation of mosaicity, since a small number of mosaicity-affected data points near T_{NA} can not significantly change the values of the critical exponents.

The critical divergence of $\xi_{\parallel,\perp}$ and σ_o in the D6.4AOB sample was also studied under different fields (5 T, 0.75 T, and 0.5 T). These studies were done using the Mo target to access a wider $q_\perp$ range. Peaks corresponding to the two,

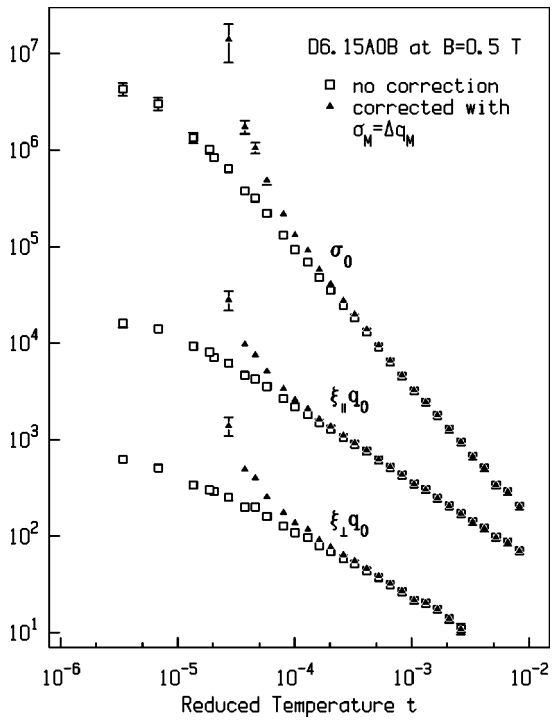

FIG. 9. Log-log plots of $q_o\xi_{\parallel,\perp}$ and σ_o vs reduced temperature t for D6.15AOB in a 0.5 T field are shown for both without a mosaicity correction and with the Gaussian mosaicity correction $\sigma_M=\Delta q_M$, where Δq_M is the width of the sharpest $q_\perp$-scan. The corrected values of $\xi_{\parallel,\perp}$ and σ_o very near T_{NA} became unrealistically large and could not be obtained because of big uncertainties ($>100\%$) and very slow convergence of the fits.

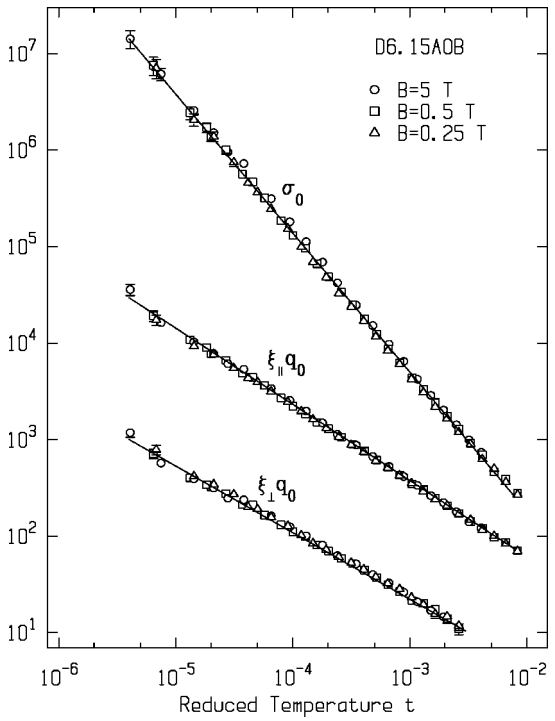

FIG. 10. Log-log plots of $q_o\xi_{\parallel,\perp}$ and σ_o vs reduced temperature t for D6.15AOB at different fields . The low-field (0.5 T and 0.25 T) data were corrected for mosaicity using the 5 T results as a reference. The appropriate Gaussian mosaicity width was found to be $\sigma_M\approx\Delta q_M/3.5$. The solid lines are the single power-law fits with the exponents given in the text.

$K\alpha_1$ and $K\alpha_2$, lines were resolved in the $q_\parallel$-scans close to the transition. The fits were obtained the same way as for the D6.15AOB sample but included one extra adjustable parameter for the intensity ratio of the two $K\alpha$ lines, while the separation between the two peaks ($\propto q_o$) was calculated. The results obtained without mosaicity correction are shown in Fig. 11, where the average T_{NA}^{fit} was only 0.4 mK away from $T_{NA}^{\exp}$. Since the Mo target gave us access to a wider $q_\perp$-range, the values of $\xi_\perp$ were not truncated at large t as in the case of the D6.15AOB sample. Unfortunately, the Mo target developed a pin-hole leak before we could perform scans at 0.25 T field, where the effects of mosaicity are most profound. The results for the D6.4AOB sample (at relatively higher fields) were not noticeably affected by the mosaicity. This is consistent with the fact that the effective transverse resolution at 0.5 T for D6.4AOB $\Delta q_M\simeq 6.0\times10^{-4}$ Å^{-1} was almost half of the value $\Delta q_M\simeq 1.1\times10^{-3}$ Å^{-1} obtained for D6.15AOB at the same field. Since the mosaicity effect at 0.5 T for D6.15AOB was already marginal and the value of t_M [$\propto(\Delta q_M)^{1/\nu_\perp}$] even smaller for D6.4AOB, the mosaicity affected regime $t\lesssim t_M$ was not accessed in our experiments for D6.4AOB. The temperature dependences of $\xi_{\parallel,\perp}$ and σ_o obtained over almost four decades of reduced temperature (the largest range of t for any x-ray study) are fit very well by single power-laws suggesting the absence of any crossover behavior as predicted by theories. The values of the critical exponents obtained for high (5 T) and low (0.5 T) fields are

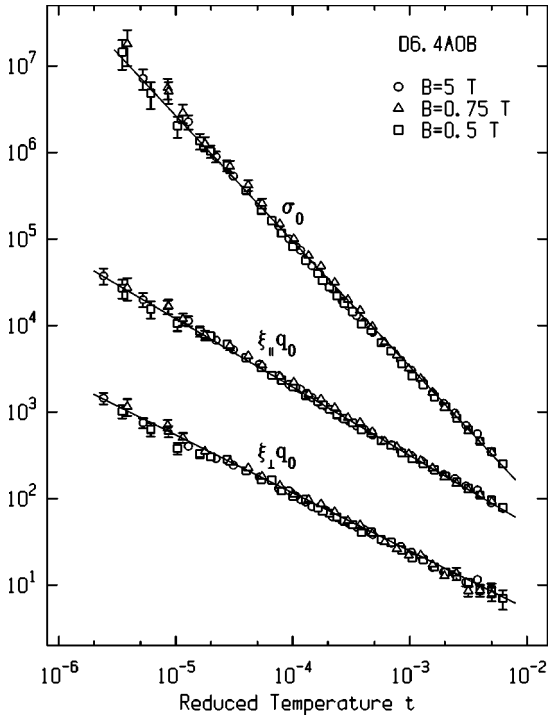

FIG. 11. Log-log plots of $q_o\xi_{\parallel,\perp}$ and σ_o vs reduced temperature t for D6.4AOB without a mosaicity correction at different fields ($q_o=0.232$ Å^{-1}). The solid lines are the single power-law fits with the exponents given in the text.

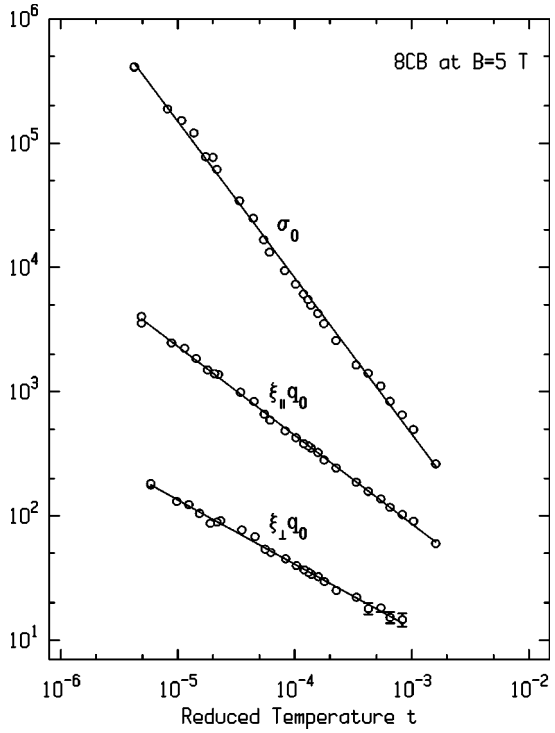

FIG. 12. Log-log plots of $q_o\xi_{\parallel,\perp}$ and σ_o vs reduced temperature t for 8CB in a 5 T field without a mosaicity correction ($q_o = 0.198$ Å^{-1}). The solid lines are the single power-law fits with the exponents given in the text.

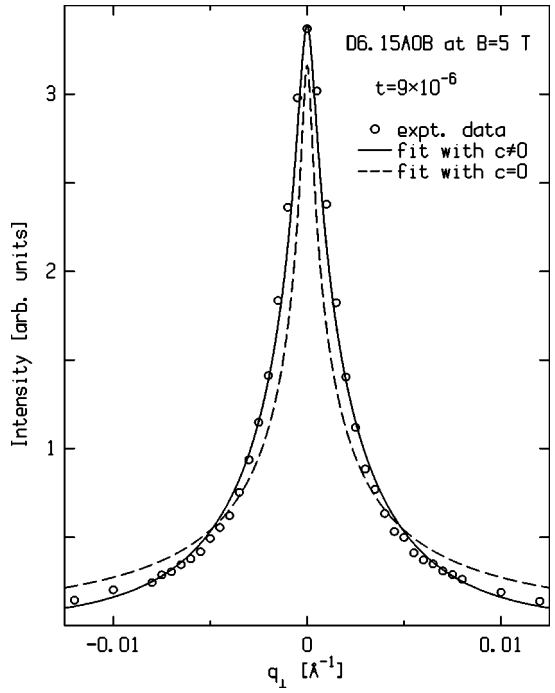

FIG. 13. The transverse in-plane $q_\perp$ scan for D6.15AOB in a 5 T field at $t=9\times10^{-6}$. The fits to the structure factor Eq. (2) convoluted with the appropriate resolution function are shown both with the fourth order coefficient c being a fitting parameter ($c \neq 0$) and with c being fixed at zero. It is clear that the $c\neq0$ fit gives a more adequate description of the experimental profile.

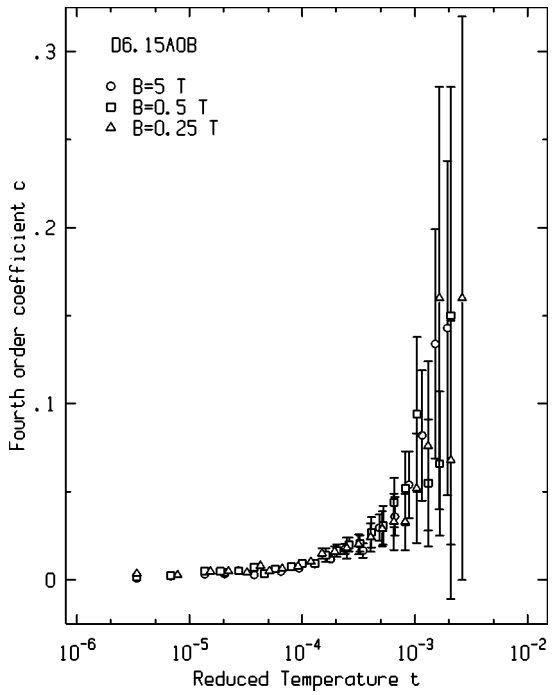

FIG. 14. The fourth order coefficient c for D6.15AOB vs reduced temperature t at different fields.

the same. This indicates that there is no noticeable effect on the critical behavior up to a field of 5 T. Finally, the values of the critical exponents, $\nu_\parallel = 0.79 \pm 0.02; \nu_\perp = 0.67 \pm 0.02$; and $\gamma = 1.44 \pm 0.04$ for D6.4AOB are the same as those for D6.15AOB within experimental errors. It appears that, far from the tricritical point, the critical exponents are the same for the two mixtures studied, and perhaps in general.

We have to admit here that critical behavior studies of the DnAOB mixtures are not complete without experimental data on heat capacity. Such data would help to understand the importance of corrections-to-scaling terms in describing the NA transition. This was pointed out by Garland *et al.* [17], who used both high-resolution x-ray diffraction and heat capacity experiments to study several SmA materials. They showed that critical behavior of the correlation volume $\xi_\parallel\xi_\perp^2$ and the susceptibility σ_o could be equally well described by simple power-law fits and fits, which use exponents fixed at $3d$-xy values and corrections-to-scaling terms fixed at the values taken from the heat capacity data and theory of correction amplitude ratios. In our data analysis we only used simple power laws to describe the critical divergence of $\xi_{\parallel,\perp}$ (and, hence, $\xi_\parallel\xi_\perp^2$) and σ_o. It would be interesting to see if the analysis from Ref. [17] holds for the DnAOB mixtures. It would also be interesting to check the validity of the hyperscaling $\nu_\parallel + 2\nu_\perp = 2 - \alpha$, which appears to be violated if the heat capacity data would show the $3d$-xy value of α.

The critical divergence of the correlation lengths and susceptibility in the 8CB sample was studied only at a 5 T field. The fits without the mosaicity correction are presented in Fig. 12, where the average T_{NA}^{fit} was 0.8 mK less than $T_{NA}^{\exp}$. The temperature dependences of $\xi_{\parallel,\perp}$ and σ_o were fit to single power laws to calculate the critical exponents $\nu_\parallel$

$=0.70\pm0.02$; $\nu_\perp=0.52\pm0.02$; and $\gamma=1.24\pm0.04$. These values are in good agreement with the previous x-ray results reported by Ocko [21] and Davidov *et al.* [25] and the results from light scattering experiments of Sprunt *et al.* [37].

Now, as we have mentioned, Dasgupta [12] suggested that the non-Lorentzian behavior of $S(q_\perp)$ in the nematic phase is related to the sample mosaicity and that a detailed experimental investigation of the effect of mosaicity on the x-ray scattering profile is required. Our experiments provide a good test of this assumption. If Dasgupta's argument were to hold, there should be a significant decrease in the values of c with increasing field. However, our studies of the three samples under 5 T field indicated that the $c\xi_\perp^4 q_\perp^4$ correction term was necessary to obtain acceptable fits (see Fig. 13). Moreover, the high- and low-field values of the coefficient c were essentially the same (see Fig. 14) ruling out any significant effects of mosaicity on the x-ray scattering profile.

VI. CONCLUSION

The critical exponents γ and $\nu_{\parallel,\perp}$ for the NA transition were measured under a strong (5 T) field in materials with both wide and narrow nematic ranges. The effective transverse resolution in a 5 T field was almost two orders of magnitude better than at low fields and was essentially the instrumental resolution. We have shown that use of a 5 T field would allow one to access three more decades of reduced temperature (up to $t\sim10^{-8}$) compared to low-field experiments before being strongly affected by mosaicity (but the oven stability sets a considerably higher limit on t). The high-field results were not affected by the mosaicity, while the effect of mosaicity on the low-field data for the D6.15AOB sample was clearly observed. The proper Gaussian mosaicity correction was found to be temperature independent but significantly (~3.5 times) smaller than the width of the sharpest $q_\perp$-scan. No significant effects of mosaicity on the values of the fourth-order coefficient c were observed. The values of the critical exponents obtained from high- and low-field experiments were the same indicating no high-field quenching of the director fluctuations. For all samples the divergence of $\xi_{\parallel,\perp}$ and σ_o over the whole range (~4 decades) of reduced temperature were fit well by single power laws. Thus, our data did not exhibit any evidence of a crossover to the strongly anisotropic regime ($\nu_\parallel=2\nu_\perp$) for $t<10^{-5}$. The values of the critical exponents for D6.15AOB and D6.4AOB were found, within experimental uncertainties, to be the same indicating that different materials with the NA transitions far from the tricritical point may have the same exponents.

ACKNOWLEDGMENTS

We would like to thank Dr. Mary Neubert and Julie Kim for synthesizing high purity materials and Professor Paul Keyes, Professor Carl Garland, and Professor Tom Lubensky for helpful discussions. This work was supported by the NSF S&T Center ALCOM Grant No. DMR-89-20147.

[1] P.G. de Gennes and J. Prost, *The Physics of Liquid Crystals* (Oxford University Press, New York, 1993).
[2] P.G. de Gennes, Solid State Commun. **10**, 753 (1972); Mol. Cryst. Liq. Cryst. **21**, 49 (1973).
[3] F.C. Frank, Discuss. Faraday Soc. **25**, 19 (1958).
[4] W.L. McMillan, Phys. Rev. A **4**, 1238 (1971); **6**, 936 (1972).
[5] K. Kobayashi, Phys. Lett. **31A**, 125 (1970); J. Phys. Soc. Jpn. **29**, 101 (1970).
[6] B.I. Halperin, T.C. Lubensky, and S.K. Ma, Phys. Rev. Lett. **32**, 292 (1974).
[7] T.C. Lubensky, J. Chem. Phys. **80**, 31 (1983).
[8] L.D. Landau, Phys. Z. Sowjetunion **11**, 545 (1937); R.E. Peierls, Helv. Phys. Acta **7**, II, 81 (1936).
[9] J. Als-Nielsen, R.J. Birgeneau, M. Kaplan, C.R. Safinya, A. Lindegaard-Andersen, and S. Mathiesen, Phys. Rev. B **22**, 312 (1980).
[10] C.W. Garland and G. Nounesis, Phys. Rev. E **49**, 2964 (1994), and references therein.
[11] C. Dasgupta and B.I. Halperin, Phys. Rev. Lett. **47**, 1556 (1981).
[12] C. Dasgupta, J. Phys. (Paris) **48**, 957 (1987).
[13] D.R. Nelson and J. Toner, Phys. Rev. B **24**, 363 (1981).
[14] T.C. Lubensky and J.-H. Chen, Phys. Rev. B **17**, 366 (1978).
[15] T.C. Lubensky, S.G. Dunn, and J. Isaacson, Phys. Rev. Lett. **47**, 1609 (1981).
[16] B.R. Patton and B.S. Andereck, Phys. Rev. Lett. **69**, 1556 (1992); B.S. Andereck and B.R. Patton, Phys. Rev. E **49**, 1393 (1994).
[17] C.W. Garland, G. Nounesis, M.J. Young, and R.J. Birgeneau, Phys. Rev. E **47**, 1918 (1993); C.W. Garland (unpublished).
[18] W.L. McMillan, Phys. Rev. A **7**, 1419 (1973).
[19] J. Als-Nielsen, R.J. Birgeneau, M. Kaplan, J.D. Litster, and C.R. Safinya, Phys. Rev. Lett. **39**, 352 (1977); **41**, 1626(E) (1978).
[20] A. Caillé, C R. Acad. Sci. III **274**, 891 (1972).
[21] B.M. Ocko, R.J. Birgeneau, and J.D. Litster, Z. Phys. B: Condens. Matter **62**, 487 (1986); B.M. Ocko, Ph.D. thesis, MIT, 1984 (unpublished).
[22] G. Nounesis, K.I. Blum, M.J. Young, C.W. Garland, and R.J. Birgeneau, Phys. Rev. E **47**, 1910 (1993).
[23] K.K. Chan, P.S. Pershan, L.B. Sorensen, and F. Hardouin, Phys. Rev. A **34**, 1420 (1986).
[24] W.G. Bouwman and W.H. de Jeu, Phys. Rev. Lett. **68**, 800 (1992); J. Phys. II **4**, 787 (1994).
[25] D. Davidov, C.R. Safinya, M. Kaplan, S.S. Dana, R. Schaetzing, R.J. Birgeneau, and J.D. Litster, Phys. Rev. B **19**, 1657 (1979).
[26] A.R. Kortan, H. von Känel, R.J. Birgeneau, and J.D. Litster, J. Phys. (Paris) **45**, 529 (1984).
[27] L. Chen, J.D. Brock, J. Huang, and S. Kumar, Phys. Rev. Lett. **67**, 2037 (1991).
[28] H.K.M. Vithana, V. Surendranath, M. Lewis, A. Baldwin, K.

Eidner, R. Mahmood, and D.L. Johnson, Phys. Rev. A **41**, 2031 (1990).
[29] W.H. de Jeu, T.W. Lathouwers, and P. Bordewijk, Phys. Rev. Lett. **32**, 40 (1974).
[30] E.F. Gramsbergen and W.H. de Jeu, J. Chem. Soc., Faraday Trans. 2 **84**, 1015 (1988).
[31] M.F. Achard, F. Hardouin, G. Sigaud, and H. Gasparoux, J. Chem. Phys. **65**, 1387 (1976).
[32] H. Marynissen, J. Thoen, and W. van Dael, Mol. Cryst. Liq. Cryst. **97**, 149 (1983); J. Thoen, H. Marynissen, and W. van Dael, Phys. Rev. Lett. **52**, 204 (1984).
[33] P.E. Cladis, W. van Saarloos, D.A. Huse, J.S. Patel, J.W. Goodby, and P.L. Finn, Phys. Rev. Lett. **62**, 1764 (1989).
[34] M.A. Anisimov, P.E. Cladis, E.E. Gorodetskii, D.A. Huse, V.I. Podneks, V.G. Taratuta, W. van Saarloos, and V.P. Voronov, Phys. Rev. A **41**, 6749 (1990).
[35] A. Yethiraj and J. Bechhoefer, Phys. Rev. Lett. **84**, 3642 (2000); Mol. Cryst. Liq. Cryst. **304**, 301 (1997); R. Mukhopadhyay, A. Yethiraj, and J. Bechhoefer, Phys. Rev. Lett. **83**, 4796 (1999).
[36] I. Lelidis, Phys. Rev. Lett. **86**, 1267 (2001).
[37] S. Sprunt, L. Solomon, and J.D. Litster, Phys. Rev. Lett. **53**, 1923 (1984).
[38] C-PLOT is a registered trademark of certified scientific software.
[39] *Mathematica* is a registered trademark of Wolfram Research.